An explicit solvent quantum chemistry study on the water environment influence on the interactions of fluoride with phenol

Piotr Cysewski,*[a] Beata Szefler,[a] Halina Szatyłowicz[b] and Tadeusz Marek Krygowski[c]

Received (in Montpellier, France) 2nd October 2008, Accepted 17th December 2008
First published as an Advance Article on the web 26th January 2009
DOI: 10.1039/b817297h

The phenol complexes with fluoride in water solution were analyzed for different F···O separation distances ranging from 2.6 Å up to 4.0 Å with 0.2 Å intervals. The quenching molecular dynamics runs were followed by hybrid quantum mechanics–molecular mechanics (QM–MM) geometry optimization at B3LYP/6–311 + G** level. The analysis of MD trajectories allowed for detailed characteristics of hydration patterns and mobility of fluoride and phenol hydroxyl group. The explicit solvent molecules taken into account in QM–MM studies impose solute geometry changes according to fluctuations of the structure of its nearest neighborhood. Hence, fluctuations of HOMA (harmonic oscillator model of aromaticity index) values were observed corresponding to different conformations of water molecules around the solute. However, the screening role of the water molecules was noticed, which reduces the influence of the fluoride compared with the gas phase. Similarly as in vapor state, also in water solution the formation of hydrogen bond between the fluoride and the hydroxyl group of phenol is energetically favorable.

Introduction

Most of the quantum-chemical modeling applied to organic molecules is devoted to computation in the gas phase[1]—and even this kind of data is often found to be in acceptable agreement with experimental data or at least with chemical intuition. However, in many cases solvent effects may affect dramatically the chemical and physicochemical properties of molecules.[2] Several excellent reviews have been published describing different theoretical foundations and applicability of modern approaches to solute–solvent interactions.[3–6] Generally, there are three alternative choices for modeling of solute properties in bulk solution. The explicit models directly take into consideration the solvent molecules. Unfortunately, such supermolecule approaches are size-limited, thus prohibiting their application to large systems at advanced levels and fully taking into account long-range effects of bulk solvent. On the other hand, much less demanding implicit solvent approaches rely only on the continuum and homogeneous medium characterized exclusively by the scalar and static dielectric constant of solvent. Although such treatments are computationally more feasible, they are unable to account for many solvent induced changes of solute properties even in dilute solutions. This is of special importance in the case of strong intermolecular interactions between solute and solvent molecules. The intermediate mixed implicit–explicit treatments or hybrid quantum mechanics–molecular mechanics (QM–MM) approaches offer real balance between the accuracy and the computational cost, since in principle they combine the correctness of a quantum mechanical description with the low computational cost of molecular mechanics. Since its first formulation,[7–9] various incorporations of quantum mechanics into molecular mechanics were proposed.[10–22] Because the partitioning of a chemical system into QM and MM regions is not straightforward, alternative approaches were formulated differing by the particular method of the calculations.[23–28] Among many realizations of QM–MM methods, the ONIOM formulation developed by Morokuma and co-workers[13–17] has reached popularity due to its high efficiency. The usefulness of QM–MM methods was demonstrated in many research areas for example thermodynamics[25,29–31] and structure of solute–solvent interactions,[32–35] description of reaction mechanisms in solutions,[36–40] acid–base equilibria,[41,42] pK_a calculations,[43–46] solvent effects on conformational change of solutes,[47–49] solvent imposed chemical shifts[50–52] and solvation structure of several metals[53–60] as for example Pb(II),[53] Cu(II),[54] Sn(II)[55] and Cr(III).[56]

The solvent molecules impose many changes on molecular properties of solutes. An interesting question arises: how dependent is a π-electron delocalization in aromatic systems on the nature of the environment? Katritzky *et al.*[61] showed by use of AM1 modeling that the aromaticity of azulene, and heteroaromatic systems such as imidazole, pyrrole, pyrazole and the like, estimated by use of the Bird aromaticity index I,[62] depends on the environment because of the changes in electric dipole moment. The changes in Bird's index were at the level of a few percent showing usually an increase of aromaticity

[a] *Department of Physical Chemistry, Collegium Medicum, Nicolaus Copernicus University, Kurpińskiego 5, 85-950 Bydgoszcz, Poland. E-mail: piotr.cysewski@cm.umk.pl*
[b] *Faculty of Chemistry, Warsaw University of Technology, Noakowskiego 3, 00-664 Warsaw, Poland*
[c] *Department of Chemistry, Warsaw University, Pasteura 1, 02-093 Warsaw, Poland*

when going from gas phase to dioxane or water. The geometry-based aromaticity index HOMA (harmonic oscillator model of aromaticity index—for review see ref. 63) was applied to the geometry of sodium[64] and magnesium[65] *p*-nitroso phenolates which differed in the number of water molecules hydrating the above-mentioned systems, three and six, respectively. This caused a dramatic change in aromaticity of the ring, from HOMA = 0.46 for sodium salt where mostly the NO group was hydrated leading to a substantial charge transfer, and in consequence to an increase of quinoid-like structure of the ring, whereas in the hexa-hydrated salt both centers of basicity were hydrated almost to the same degree, and hence much less quinoid-like structure of the ring appeared and HOMA was 0.63.[66] For comparison, HOMA = 0 for the Kekule structure of benzene and 1 for benzene itself.[67]

The aim of this paper is to show how various molecular parameters like bond lengths, rotation of OH and OH$\cdots$F$^-$ groups, aromatic character of the ring and others in phenol H-bonded complexes with fluoride and a varying H-bond strength are changed as a result of a "solvent effect" in the sense of solute–solvent interactions.

Methods

The two-step procedure was applied for structural and energetic characteristics of phenol complexes with fluoride in water solution. The quenching molecular dynamics runs were followed by hybrid QM–MM geometry optimization. The first stage provided conformation fluctuations, whereas the second one was used for estimation of the geometric pattern and then the values of structural index of aromaticity, HOMA. Before the MD was run, the atomic charges were calculated according to the Merz–Kollman scheme *via* the RESP procedure[68] at B3LYP/6–311+G** level. Each separation distance between fluoride and the oxygen atom of the phenol was analyzed separately, and small but systematic variations of point atomic charges were noticed. Thus, the potential induction of the electrostatic field of anion on the neutral molecule was taken into account. The AMBER force field[69] was used for dynamic trajectory generation. The model system consisted of one phenol molecule placed in the middle of a 60 $\times$ 60 $\times$ 60 Å cube. The box was filled with 5832 water molecules of TIP3P type.[70] The fluoride was placed at the controlled distance from the oxygen atom of the phenol. The F$\cdots$O separation distance was fixed during all molecular dynamics runs at values ranging from 2.6 Å up to 4.0 Å with 0.2 Å interval. The periodic boundary conditions were applied at room temperature. After initial equilibration the 500 ps long runs were performed for each of F$\cdots$O separation distance. All the systems readily underwent equilibration. Stable fluctuations of root mean square deviations (RMSD) as well as total, potential and kinetic energies were usually achieved just after 20 ps. Starting from 100 ps collection of snapshots was performed every 1 ps for each run corresponding to different F–O separations. The resulting conformations were pre-optimized based on AMBER force field, and only low-energy structures were selected for further hybrid QM–MM calculations.[71,72] The criterion was set to 10 kcal mol^{-1} with respect to the lowest energy snapshot. Before the ONIOM[13–17] hybrid calculations were performed, each system was divided into two layers, namely HIGH quantum chemistry layer (B3LYP/6–311+G**) and LOW molecular mechanics layer (AMBER force field). The HIGH layer comprised phenol, fluoride and nine water molecules in the nearest proximity to F$^-$, as schematically presented in Fig. 1. The rest of the water molecules were defined as LOW layer. All hybrid calculations were performed based on Gaussian03,[73] whereas molecular dynamics calculations were done using Amber 8.0 software.[74]

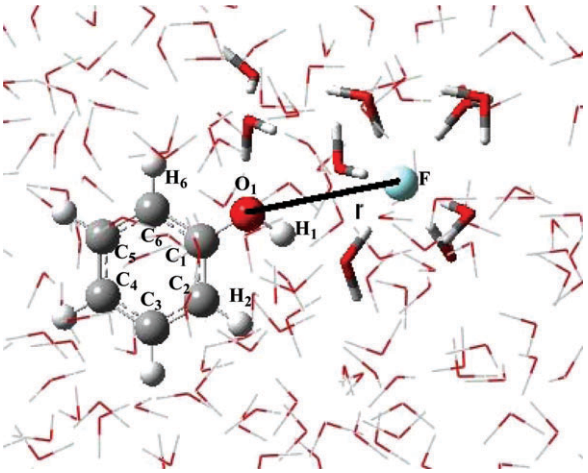

Fig. 1 The definition of the fluoride–phenol system for QM–MM modeling. The fluoride along with phenol and the water molecules marked by thick tubes define the HIGH layer treated on quantum chemistry level. The rest of the water molecules (thin tubes) are within the LOW layer analyzed *via* MM–AMBER force field.

Results and discussion

Dynamic properties (MD runs)

The molecular dynamics runs performed for nine O$\cdots$F separation distances allowed us to make a detailed interpretation of the system behavior. The hydration patterns and the mobility of particular fragments are directly available from each trajectory.

Hydration of phenol and fluoride

The fluctuations of water molecules in immediate vicinity of the analyzed system are a main source of the observed structural and energetic heterogeneities. Thus, the hydration patterns are analyzed in the first place. Fig. 2 presents the mean numbers of water molecules found within a defined distance from either the center of aromatic ring or fluoride. The selection radius was set to 3.0 Å and 4.0 Å, which corresponds to the expected first and second solvation layers, respectively. Interestingly, fluoride is highly solvated and on average about five water molecules are tightly bound *via* short and strong hydrogen bonds. Such interactions of water molecules are only slightly dependent on the F$\cdots$O$_1$ separation distance. For the shortest distance, the mean number of water molecules around the fluoride is about 3.5 within 3.0 Å and almost 5 for a sphere of 4.0 Å radius. Interestingly, these values are smaller in comparison with free fluoride in water, for which the expected coordination number is equal to six.

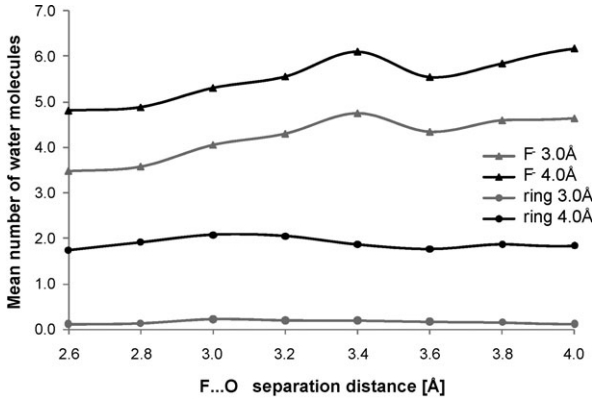

Fig. 2 The hydration layers formed around fluoride and the aromatic ring of phenol characterized as the mean value of water molecules estimated for each molecular dynamics run.

This represents the existence of $[F(H_2O)]_6^-$ anion in water solution. As may be inferred from Fig. 2, such a complex may be formed for separation distances high enough since the mean number of water molecules in the 4.0 Å proximity to fluoride is about six in the case of 4.0 Å separation between the anion and oxygen atom of the hydroxyl group of phenol molecule. If fluoride is in a closer proximity to the hydroxyl group, there is not enough room for full hydration and the number of water molecules decreases to 5. The hydroxyl group of phenol is expected to interact with six water molecules. The hydrophobic ring of benzene is not hydrated, except the one water molecule above each side of the plane of the ring. Such a description of hydration of the analyzed system is in good agreement with chemical intuition, confirming the reliability of the applied model.

Impact of fluoride proximity on the hydroxyl group mobility

It is reasonable to expect that the interactions of fluoride with the hydroxyl group of phenol should affect the mobility of the latter. Indeed, this is demonstrated in Fig. 3 by fluctuations of $F\cdots H_1$ distances over time presented for different values of $F\cdots O_1$ coordinate. At far remoteness of the fluoride, the range of fluctuations of $F\cdots H_1$ values is large and frequently increases up to 1 Å. This demonstrates almost unperturbed rotation of the hydroxyl group. It is worth remembering that the $F\cdots O_1$ distance is kept fixed during simulations. The closer the fluoride is to the oxygen atom of the phenol, the more significant is the fixing of H_1 hydrogen atom of the hydroxyl group with respect to the approaching anion. The smallest variations of the $F\cdots H_1$ coordinate are of course observed if strong binding of fluoride takes place. In the case of $F\cdots O_1$ distance equal to 2.6 Å or 2.8 Å, the variations are within thermal fluctuations of phenol hydroxyl group. This indicates that hydrogen atom is almost in the line between oxygen and fluoride. At $F\cdots O_1$ separation equal to 3.0 Å, the mobility of the H_1 hydrogen atom becomes important, and at slightly further separations ($\geq$3.2 Å) the $F\cdots H_1$ hydrogen bond is no longer expected to form. It is interesting to know if such behavior of the H_1 atom is accompanied by corresponding rotation of the hydroxyl group. Fig. 4a presents the time evolution of C_2–C_1–O_1–H_1 torsion angle (numbering of the atoms in Fig. 1) for the nearest proximity of fluoride. Clearly, there are two preferential conformations of the hydroxyl group, which may be interpreted as *syn* and *anti* orientations of OH with respect to the C_2 atom of the ring. Obviously, rotation of the OH group occurs during MD simulations, but two positions are favored, which are roughly coplanar with the benzene moiety. Keeping in mind that a strong hydrogen bond is formed between fluoride and the H_1 atom at this separation distance (see Fig. 3), the intriguing movement of fluoride must

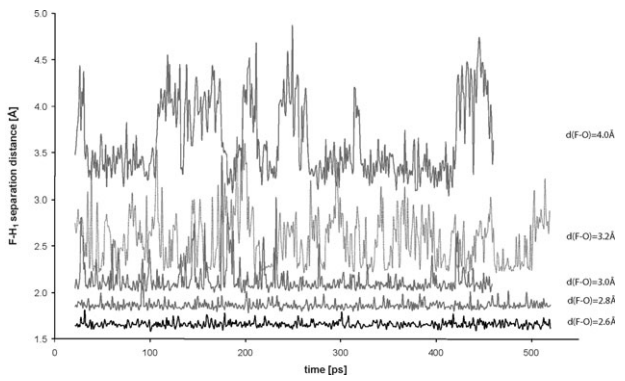

Fig. 3 Fluctuations of $F\cdots H_1$ separation distance as a function of time for five distinct MD runs corresponding to different values of $F\cdots O_1$ coordinate.

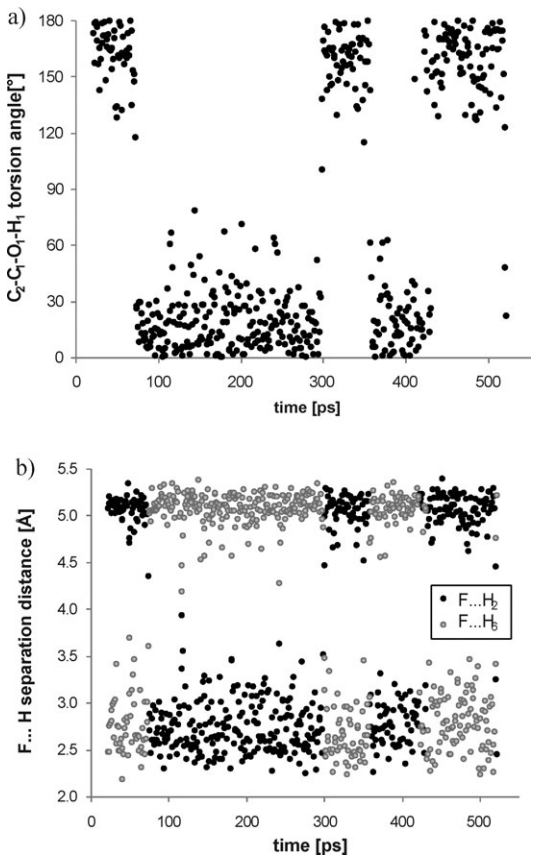

Fig. 4 Time evolution of selected coordinates defining orientation of the hydroxyl group of phenol, C_2–C_1–O_1–H_1 torsion angle, (a) and the position of fluoride with respect to phenol, $F\cdots H_2$ and $F\cdots H_6$, (b) in the case of $d(F\cdots O_1)$ = 2.6 Å.

be accomplished with the rotation of the hydroxyl group. Indeed, the analysis of time evolution of F···H_2 and F···H_6 (numbering of atoms in Fig. 1) separation distances coming from the trajectory corresponding to F···O_1 distance equal to 2.6 Å (Fig. 4b), leads to the conclusion that there is a direct correlation between rotation of the OH group and the movement of fluoride. In this case, the hydrogen bond formed *via* the F···H_1–O_1 bridge is so strong that spontaneous flipping of fluoride occurs. At higher F···O_1 separations, where the interactions of fluoride with the hydroxyl group of the phenol molecule become screened by water molecules, this behavior is not observed.

Mobility of fluoride

The final comment on the dynamic properties of the system analyzed is related to the path of dissociation of the F···H_1 hydrogen bond. In the gas phase, the fluoride is able to interact with the H_2 atom forming a bifurcated structure. The same possibility is also observed in water solutions. As a measure of the dissociation path the values of the F···H_1–O_1 angle may be chosen. In Fig. 5 the fluctuations of the values of this angle as well as averaged data are presented. The inspection of these data leads to the conclusion that fluoride still interacts with the phenol molecule even at relatively large separation distances. This justifies a significant reduction of the F···H_1–O_1 angle along the dissociation path. Interestingly, at 4.0 Å separation distance, between fluoride and the oxygen atom, the fluctuations of the F···H_1–O_1 angle indicate oscillations of fluoride toward the hydrogen atom in the *ortho* position. On the contrary, in close proximity of the fluoride and formations of the strong hydrogen bond with the OH group, the average value of F···H_1–O_1 angle is close to 170°. A systematic decrease of these parameters is observed as the fluoride departs from the phenol system.

Structural properties (QM–MM study)

It is well known that polar solvents screen electrostatic interactions. One of the measures of such an effect is the value of the dielectric constant (ε). For example, in the case of water $\varepsilon = 78.5$, which means that the electrostatic interactions between point charges are about 80 times weaker in water environment than in vacuum, if placed at the same distances. Consequently, it is reasonable to expect that the impact of the fluoride on the phenol aromaticity should be manifested to a lesser extent in water solutions than in the vapor state. A question immediately arises: which of the contemporary solvation models is reliable enough to describe these phenomena? Out of many possibilities, the explicit models seem to be the best to choose since the polarized continuum solvation models often overestimate the relaxation of molecular geometries. One of the most spectacular examples is 4-NO-aniline, for which the HOMA value changes from 0.922 in vapor at B3LYP/6–311+G** level to 0.735, if estimated by the IEFPCM model at the same level of theory.[75,76] The observed over 25% reduction of the aromatic character is rather a method artifact than an experimentally confirmed property of this compound. On the other hand, for most of the aromatic species much less reduction of aromaticity is observed if the PCM model is used. Thus, despite its inherent shortcoming the PCM models may still offer valuable reference data. The explicit solvent models are beneficial due to direct involvement of the solute–solvent interactions. However, it is worth mentioning that the TIP3P model of water molecules overestimates[77,78] hydrogen bond interaction between the solute in QM layer and solvent molecules belonging to MM part. In our model, all water molecules within 3 Å radius from a hydroxyl group of either phenol or fluoride anion were treated on QM level. Thus, such a drop of water in the nearest vicinity to fluoride interacting with phenol is in fact treated as "extended" solute. Of course, the water model still affects the structure of solvent molecules in the solute neighborhood. However, in our QM–MM model the actual interactions inside such "extended" solute are treated on the QM level rather than MM. It is reasonable to expect that careful selection of the size of the first hydration layer reduces artifacts related to QM and MM frontiers. Some tests not mentioned in the text were performed prior to actual calculations for different radii of the first solvation layer. The results led to the conclusion that increasing the number of water molecules in the HIGH level did not affect significantly the structural and energetic properties of the system analyzed. Furthermore, a serious problem arises as concerns the selection of meaningful conformations of solvent molecules around the solute

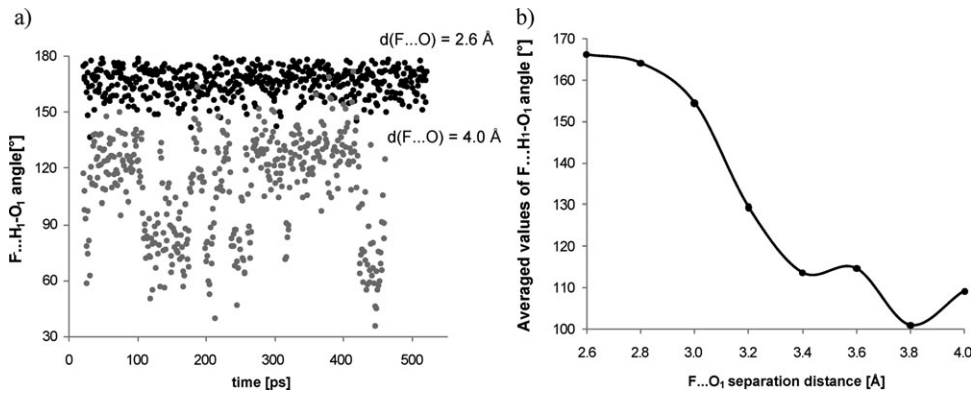

Fig. 5 The fluctuations of F···H_1–O_1 angle observed during MD simulations corresponding to two selected separation distances of F···O_1 (a) and averaged values of this angle estimated for all the analyzed trajectories (b).

molecule. One of the frequently used ways is the so-called quenching method, which takes snapshots from molecular dynamics runs and uses them as initial conformations for quantum chemistry calculations. This is a very promising way if combined with hybrid quantum chemistry–molecular mechanics methods, QM–MM. The solute along with a few solvent molecules may be treated on an advanced quantum chemistry level, while the rest of the solution may be mimicked by explicit solvent within the MM framework. The definition of these two regions may be based on chemical intuition and adjusted according to a particular situation. Such a treatment has simple chemical meaning and potentially may be implemented for any kind of system. There is also an intermediate way, which is a combination of the above two and is sometimes referred to as the microsolvated model. According to this approach, the solute and a few explicit solvent molecules are calculated as supermolecule either in vapor or within the PCM framework. Again the source of particular conformation may be the quenching MD runs.

Below there are presented and discussed the results of the first two methods. In Fig. 6 the values of HOMA are plotted against the F···O_1 separation distance. The dotted line represents the impact of the fluoride on the structural aromaticity index in the gas phase. The results of analogous calculations performed in the implicit water solution within the IEFPCM model are plotted as a solid black curve in Fig. 6. The expected systematic reduction of aromaticity is observed in the latter case for all separation distances of F···O_1. The last set of data presented in Fig. 6 corresponds to the QM–MM ONIOM model. Interestingly, the fluctuations of HOMA values were observed corresponding to different conformations of water molecules around the solute. The explicit solvent molecules impose solute geometry changes according to fluctuations of the structure of its nearest neighborhood. This expresses the inherent feature of any real system comprising the interactions of discrete molecules. The averaged values, presented in Fig. 6 as the gray line, correspond to much higher HOMA values than the ones estimated based on the IEFPCM model. The observed fluctuations are the smallest in the case of high separation distance of fluoride and at the same time the

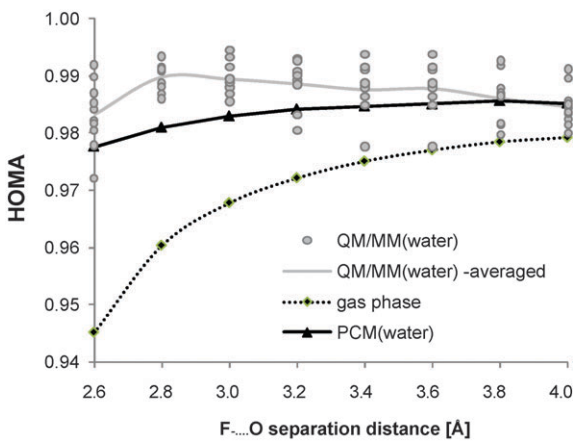

Fig. 6 The values of structural measure of aromaticity, HOMA, as the function of F···O_1 separation distance estimated by QM and QM–MM quantum chemistry studies at B3LYP/6–311+G** level.

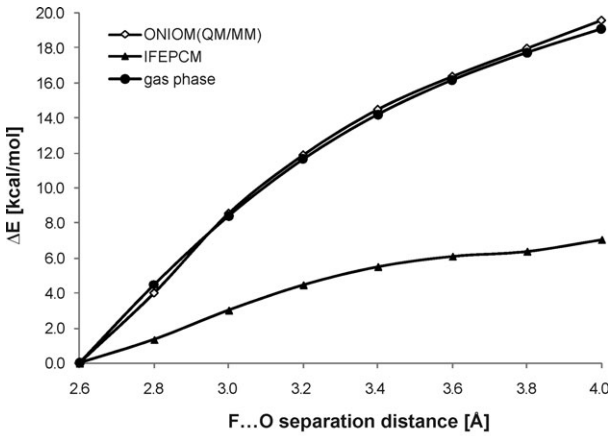

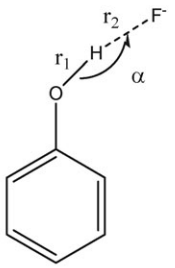

F…O	r_1	α	r_2
2.6	1.002	177.4	1.599
2.8	0.982	167.2	1.834
3.0	0.974	171.1	2.034
3.2	0.968	161.4	2.268
3.4	0.969	161.1	2.469
3.6	0.968	149.5	2.733
3.8	0.989	144.7	3.100
4.0	0.990	143.6	3.159

Fig. 7 Structural and energetic properties of the lowest energy conformations of the analyzed QM–MM systems. The values of distances and angles are expressed in Angstroms and degrees, respectively.

predictions of PCM and ONIOM models are almost identical. Fig. 7 presents structural and energetic properties of conformations corresponding to the lowest values of total energy. It shows that the formation of a hydrogen bond between the fluoride and the hydroxyl group of phenol is energetically favorable in water. The energy penalty for breaking this hydrogen bond equals at least 22 kcal mol^{-1}.

As the F···H_1 distance increases, there is a visible shortening of the H_1–O_1 bond, which corresponds to the release of interaction of phenol with fluoride. However, inspection of the values of the F···H_1–O_1 angle suggests that the H_1–O_1 bond does not define the direction of the fluoride withdrawal. On the contrary, within the analyzed F···O_1 distances, the values of the F···H_1–O_1 angle decrease, which is accomplished with interactions of fluoride with the *o*-hydrogen atom of phenol. This aspect was also revealed by analysis of the molecular dynamics trajectories.

The influence of the fluoride approaching the phenol molecule on the C_1–O_1 bond length is presented in Fig. 8. Interestingly, distinct features are manifested in the gas phase and in water solution. In the vapor state there is observed a smooth and monotonous increase of the C_1–O_1 bond. However, the path of fluoride separation influences the length of this bond. In the case when the fluoride is carried away along the F···H_1–O_1 line, a shortening of the C_1–O_1 bond is observed as compared with free stray away of F^- at the corresponding fluoride separation distances. If the F···H_1–O_1 angle is kept constant at 180°, no bifurcate-like interactions of fluoride are allowed with H_2 or H_6 hydrogen atoms. In this

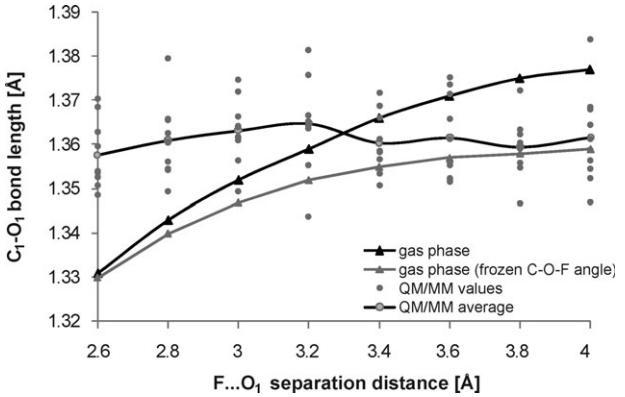

Fig. 8 The impact of $F\cdots O_1$ separation distance on the C_1–O_1 bond length estimated for a broad range of fluoride–phenol proximities. The QM–MM structures are the source of all geometric parameters in water solution and B3LYP/6–311G** results for gas phase related data.

case the C_1–O_1 bond varies from 1.330 Å to 1.359 Å within the studied range of fluoride proximities. If the values of $F\cdots H_1$–O_1 angle are freely optimized, the elongation of C_1–O_1 bond is visible and the corresponding interval spans from 1.331 Å to 1.377 Å. Interestingly, in water solution modeled within the explicit solvent model, the configuration-dependent alterations of the C_1–O_1 bond take place. The averaged values of this bond, plotted as a gray line in Fig. 8, have a monotonous trend only for immediate vicinity of fluoride. Starting from 3.2 Å separation of fluoride a slight decrease of the C_1–O_1 bond is observed. However, these changes are within standard deviation, which is equal to 0.008 Å. Thus, the screening of water molecules is evident, and from the statistical point of view the populations of C_1–O_1 bonds are the same for different $F\cdots O_1$ separations. Thus, an almost insignificant impact of the fluoride proximity on the C_1–O_1 length is to be expected in water.

Conclusions

Most changes in bond lengths of a solute are related to specific interactions of water molecules with charged parts of the system studied. The direct inclusion of water molecules, even only those forming the first solvation layer, significantly affects the analyzed solute. Moreover, the conformation changes of explicit water molecules found in the nearest neighborhood of phenol impose structural fluctuations on the solute. This, in turn, leads to fluctuations of aromaticity described by the structural index. The second role of solvent molecules is the screening of electrostatic interactions reducing the influence of ions on the solute in comparison with the gas phase. The highly polar and polarizable water molecules are particularly active, significantly isolating the fluoride electrostatic field from phenol. The dynamic properties inferred from trajectory analysis also give insight into the behavior of the analyzed solute in water solution. For long $F\cdots O$ distance the hydroxyl group rotates almost freely; when the distance becomes shorter, there appears a relatively strong H-bond between hydrogen atom of the hydroxyl group and fluoride. This kind of interaction is so strong that at short distance rotation of the $O–H\cdots F^-$ group was observed. Thus, the quenching MD simulations accomplished with QM–MM geometry optimizations provide a promising way for the dynamic, structural and energetic description of model bulk systems. Although this approach is in good accord with chemical intuition, the careful definition of applied model is indispensable for reducing potential shortcomings and inherent method-related artifacts.

References

1 S. M. Bachrach, *Computational Organic Chemistry*, J. Wiley & Sons Inc., Hoboken, New Jersey, 2007.
2 C. Reichardt, *Solvent Effects in Organic Chemistry, Third, updated and enlarged edition*, Wiley-VCH, Weinheim, 2003.
3 *Computer Simulation of Biomolecular Systems. Theoretical and Experimental Applications*, ed. W. F. Van Gunsteren, P. K. Weiner and A. J. Wilkinson, Kluwer, Dordrecht, 1997, vol. 3.
4 C. J. Cramer and D. G. Truhlar, *Chem. Rev.*, 1999, **99**, 2161.
5 M. Orozco and F. J. Luque, *Chem. Rev.*, 2000, **100**, 4187.
6 J. Tomasi, B. Mennucci and R. Cammi, *Chem. Rev.*, 2005, **105**, 2999.
7 A. Warshel and M. Levitt, *J. Mol. Biol.*, 1976, **103**, 22.
8 U. C. Singh and P. A. Kollman, *J. Comput. Chem.*, 1986, **7**, 718.
9 M. J. Field, P. A. Bash and M. Karplus, *J. Comput. Chem.*, 1990, **11**, 700.
10 J. Gao, *J. Phys. Chem.*, 1992, **96**, 537.
11 J. Gao, *Acc. Chem. Res.*, 1996, **29**, 298.
12 J. Gao, P. Amara, C. Alhambra and M. J. Field, *J. Phys. Chem. A*, 1998, **102**, 4714.
13 F. Maseras and K. Morokuma, *J. Comput. Chem.*, 1995, **16**, 1170.
14 M. Svensson, S. Humbel, R. D. J. Froese, T. Matsubara, S. Sieber and K. Morokuma, *J. Phys. Chem.*, 1996, **100**, 19357.
15 S. Dapprich, I. Komaromi, K. S. Byun, K. Morokuma and M. J. Frisch, *J. Mol. Struct. (THEOCHEM)*, 1999, **461**, 1.
16 T. Vreven, K. Morokuma, O. Farkas, H. B. Schlegel and M. J. Frisch, *J. Comput. Chem.*, 2003, **24**, 760.
17 T. Vreven, K. S. Byun, I. Komaromi, S. Dapprich, J. A. Montgomery, K. Morokuma and M. J. Frisch, *J. Chem. Theor. Comput.*, 2006, **2**, 815.
18 T. Kerdcharoen and K. Morokuma, *Chem. Phys. Lett.*, 2002, **355**, 257.
19 A. Tongraar, K. R. Liedl and B. M. Rode, *J. Phys. Chem. A*, 1998, **102**, 10340.
20 X. Assfeld and J. L. Rivail, *Chem. Phys. Lett.*, 1996, **263**, 100.
21 N. Reuter, A. Dejaegere, B. Maigret and M. Karplus, *J. Phys. Chem.*, 2000, **104**, 1720.
22 C. Bo and F. Maseras, *Dalton Trans.*, 2008, 2911.
23 T. Vreven and K. Morokuma, Hybrid Methods ONIOM(QMMM) and QM/MM, in *Annual Reports in Computational Chemistry*, pp. 35–50, vol. 2, DOI 10.1016/S1574-1400(06)02003-2, ch. 3.
24 J. Gao, *Rev. Comput. Chem.*, 1996, **7**, 119.
25 J. Gao and D. G. Truhlar, *Annu. Rev. Phys. Chem.*, 2002, **53**, 467.
26 R. A. Friesner and V. Guallar, *Annu. Rev. Phys. Chem.*, 2005, **56**, 389.
27 H. Lin and D. G. Truhlar, *Theor. Chem. Acc.*, 2007, **117**, 185.
28 H. M. Senn and W. Thiel, *Top. Curr. Chem.*, 2007, **268**, 173.
29 T. Horia, H. Takahashia, M. Nakanoa, T. Nittaa and W. Yangb, *Chem. Phys. Lett.*, 2006, **419**(1–3), 240.
30 E. Rosta, M. Klähn and A. Warshel, *J. Phys. Chem. B*, 2006, **110**(6), 2934.
31 V. I. Danilov, T. van Mourik and V. I. Poltev, *Chem. Phys. Lett.*, 2006, **429**, 255.
32 R. B. Murphy, D. M. Philipp and R. A. Friesner, *J. Comput. Chem.*, 2000, **21**, 1442.
33 V. Vchirawongkwin, B. M. Rode and I. Persson, *J. Phys. Chem. B*, 2007, **111**, 4150.
34 M. Q. Fatmi, T. S. Hofer, B. R. Randolf and B. M. Rode, *J. Phys. Chem. B*, 2007, **111**(1), 151.
35 D. E. Bikiel, F. Di Salvo, M. C. G. Lebrero, F. Doctorovich and D. A. Estrin, *Inorg. Chem.*, 2005, **44**(15), 5286.
36 Y. Zhang, H. Liu and W. Yang, *J. Chem. Phys.*, 2000, **112**, 3483.

37 V. Gogonea, L. M. Westerhoff and K. M. Merz, *J. Chem. Phys.*, 2000, **113**, 5604.
38 R. J. Hall, S. A. Hindle, N. A. Burton and I. H. Hillier, *J. Comput. Chem.*, 2000, **21**, 1433.
39 J. Sauer and M. Siekka, *J. Comput. Chem.*, 2000, **21**, 1470.
40 N. Reuter, A. Dejaegere, B. Maigret and M. Karplus, *J. Phys. Chem. A*, 2000, **104**, 1720.
41 Q. Cui, M. Elstner, E. Kaxiras, T. Frauenheim and M. Karplus, *J. Phys. Chem. B*, 2001, **105**, 569.
42 D. Gao, P. Svoronos, P. K. Wong, D. Maddalena, J. Hwang and H. Walker, *J. Phys. Chem. A*, 2005, **109**, 10776.
43 P. A. Kollman, *Chem. Rev.*, 1993, **93**, 2395.
44 M. Yoda, Y. Inoue and M. Sakurai, *J. Phys. Chem. B*, 2003, **107**, 14569.
45 G. Li and Q. Cui, *J. Phys. Chem. B*, 2003, **107**, 14521.
46 J. H. Jensen, H. Li, A. D. Robertson and P. A. Molina, *J. Phys. Chem. A*, 2005, **109**, 6634.
47 H. Sato and F. Hirata, *J. Mol. Struct. (THEOCHEM)*, 1999, **113**, 461.
48 T. Ishida, F. Hirata and S. Kato, *J. Chem. Phys.*, 1999, **110**, 3938.
49 A. V. Nemukhin, B. L. Grigorenko, A. V. Bochenkova, V. M. Kovba and E. M. Epifanovsky, *Struct. Chem.*, 2004, **15**(1), 3.
50 T. Yamazaki, H. Sato and F. Hirata, *Chem. Phys.*, 2000, **325**, 668.
51 T. Yamazaki, H. Sato and F. Hirata, *J. Chem. Phys.*, 2001, **115**, 8949.
52 S. Komin, C. Gossens, I. Tavernelli, U. Rothlisberger and D. Sebastiani, *J. Phys. Chem. B*, 2007, **111**, 5225.
53 T. S. Hofer and B. M. Rode, *J. Chem. Phys.*, 2004, **121**, 6406.
54 C. F. Schwenk and B. M. Rode, *ChemPhysChem*, 2004, **5**, 342.
55 T. S. Hofer, A. B. Pribil, B. R. Randolf and B. M. Rode, *J. Am. Chem. Soc.*, 2005, **127**, 14231.
56 C. Kritayakornupong, K. Plankensteiner and B. M. Rode, *J. Comput. Chem.*, 2004, **25**, 1576.
57 T. S. Hofer, B. R. Randolf and B. M. Rode, *J. Phys. Chem. B*, 2008, **112**(37), 11726.
58 A. Tongraar, K. Sagarika and B. M. Rode, *Phys. Chem. Chem. Phys.*, 2002, **4**, 628.
59 T. Kerdcharoen, K. R. Liedl and B. M. Rode, *Chem. Phys.*, 1996, **211**, 313.
60 M. Q. Fatmi, T. S. Hofer, B. R. Randolf and B. M. Rode, *Phys. Chem. Chem. Phys.*, 2006, **8**, 1675.
61 A. R. Katritzky, M. Karelson and A. P. Wells, *J. Org. Chem.*, 1996, **61**, 1619.
62 C. W. Bird, *Tetrahedron*, 1992, **48**, 335.
63 T. M. Krygowski and M. K. Cyrański, *Chem. Rev.*, 2001, **101**, 1385.
64 H. J. Talberg, *Acta Chem. Scand.*, 1977, **A31**, 37.
65 H. J. Talberg, *Acta Chem. Scand.*, 1975, **A29**, 919.
66 T. M. Krygowski, *J. Chem. Inf. Comput. Sci.*, 1993, **33**, 70.
67 T. M. Krygowski, A. Ciesielski, C. W. Bird and A. Kotschy, *J. Chem. Inf. Comput. Sci.*, 1995, **35**, 203.
68 J. Wang, P. Cieplak and P. A. Kollman, *J. Comput. Chem.*, 2000, **21**, 1049.
69 J. Wang, R. M. Wolf, J. W. Caldwell, P. A. Kollamn and D. A. Case, *J. Comput. Chem.*, 2004, **25**, 1157.
70 W. L. Jorgensen, J. Chandrasekhar, J. Madura and M. L. Klein, *J. Chem. Phys.*, 1983, **79**, 926.
71 S. Humbel, S. Sieber and K. Morokuma, *J. Chem. Phys.*, 1996, **105**, 1959.
72 M. Svensson, S. Humbel and K. Morokuma, *J. Chem. Phys.*, 1996, **105**, 3654.
73 M. J. Frisch, G. W. Trucks, H. B. Schlegel, G. E. Scuseria, M. A. Robb, J. R. Cheeseman, J. A. Montgomery, Jr, T. Vreven, K. N. Kudin, J. C. Burant, J. M. Millam, S. S. Iyengar, J. Tomasi, V. Barone, B. Mennucci, M. Cossi, G. Scalmani, N. Rega, G. A. Petersson, H. Nakatsuji, M. Hada, M. Ehara, K. Toyota, R. Fukuda, J. Hasegawa, M. Ishida, T. Nakajima, Y. Honda, O. Kitao, H. Nakai, M. Klene, X. Li, J. E. Knox, H. P. Hratchian, J. B. Cross, V. Bakken, C. Adamo, J. Jaramillo, R. Gomperts, R. E. Stratmann, O. Yazyev, A. J. Austin, R. Cammi, C. Pomelli, J. W. Ochterski, P. Y. Ayala, K. Morokuma, G. A. Voth, P. Salvador, J. J. Dannenberg, V. G. Zakrzewski, S. Dapprich, A. D. Daniels, M. C. Strain, O. Farkas, D. K. Malick, A. D. Rabuck, K. Raghavachari, J. B. Foresman, J. V. Ortiz, Q. Cui, A. G. Baboul, S. Clifford, J. Cioslowski, B. B. Stefanov, G. Liu, A. Liashenko, P. Piskorz, I. Komaromi, R. L. Martin, D. J. Fox, T. Keith, M. A. Al-Laham, C. Y. Peng, A. Nanayakkara, M. Challacombe, P. M. W. Gill, B. Johnson, W. Chen, m. W. Wong, C. Gonzalez and J. A. Pople, *GAUSSIAN 03 (Revision A.1.)*, Gaussian, Inc., Wallingford, CT, 2004.
74 D. A. Case, T. A. Darden, T. E. Cheatham III, C. L. Simmerling, J. Wang, R. E. Duke, R. Luo, K. M. Merz, B. Wang, D. A. Pearlman, M. Crowley, S. Brozell, V. Tsui, H. Gohlke, J. Mongan, V. Hornak, G. Cui, P. Beroza, C. Schafmeister, J. W. Caldwell, W. S. Ross and P. A. Kollman, *AMBER 8*, University of California, San Francisco, 2004.
75 J. Tomasi, B. Mennucci and E. Cancès, *J. Mol. Struct. (THEOCHEM)*, 1999, **464**, 211.
76 B. Mennucci, E. Cancès and J. Tomasi, *J. Phys. Chem. B*, 1997, **101**, 10506.
77 J. Tu and A. Laaksonen, *J. Chem. Phys.*, 1999, **111**, 7519.
78 J. Tu and A. Laaksonen, *J. Chem. Phys.*, 2000, **113**, 11264.